Journal of Microbiology (2014) Vol. 52, No. 11, pp. 898–907
DOI 10.1007/s12275-014-4075-3

Spatial Distribution of Microbial Communities Associated with Dune Landform in the Gurbantunggut Desert, China[§]

Ruyin Liu[1], Ke Li[1], Hongxun Zhang[1*], Junge Zhu[2], and DevRaj Joshi[3]

[1]*University of Chinese Academy of Sciences, Beijing 100049, P. R. China*
[2]*Institute Of Microbiology, Chinese Academy of Sciences, Beijing, 100101, P. R. China*
[3]*Research Center for Eco-Environmental Sciences, Chinese Academy of Sciences, Beijing, 100085, P. R. China*

(Received Feb 7, 2014 / Revised Mar 14, 2014 / Accepted May 7, 2014)

The microbial community compositions and potential ammonia oxidation in the topsoil at different positions of sand dune (stoss slope, crest, lee slope, and interdune) from the Gurbantunggut Desert, the largest semi-fixed desert in China, were investigated using several molecular methods. Actinobacteria and Proteobacteria (especially Alphaproteobacteria) were commonly the dominant taxa across all soil samples. Bacterial communities were similar in soils collected from the stoss slopes and interdunes (HC-BSCs, biological soil crusts with a high abundance of cyanobacteria), containing more abundant cyanobacterial populations (16.9–24.5%) than those (0.2–0.7% of Cyanobacteria) in the crests and lee slopes (LC-BSCs, biological soil crusts with a low abundance of cyanobacteria). The Cyanobacteria were mainly composed of *Microcoleus* spp., and quantitative PCR analysis revealed that 16S rRNA gene copy numbers of Cyanobacteria (especially genus *Microcoleus*) were at least two orders of magnitude higher in HC-BSCs than in LC-BSCs. Heterotrophic *Geodermatophilus* spp. frequently occurred in HC-BSCs (2.5–8.0%), whereas genera *Arthrobacter*, *Bacillus*, and *Segetibacter* were significantly abundant in LC-BSC communities. By comparison, the desert archaeal communities were less complex, and were dominated by *Nitrososphaera* spp. The *amoA* gene abundance of ammonia-oxidizing archaea (AOA) was higher than that of ammonia-oxidizing bacteria (AOB) in all soil samples, particularly in the interdunal soils (10^6–10^8 archaeal *amoA* gene copies per gram dry soil), indicating that AOA possibly dominate the ammonia oxidation at the interdunes.

Keywords: Gurbantunggut Desert, microbial community, ammonia oxidation

*For correspondence. E-mail: hxzhang@ucas.ac.cn; Tel. & Fax: +86-10-88256151
[§]Supplemental material for this article may be found at http://www.springerlink.com/content/120956.

Introduction

In desert ecosystems, highly specialized organisms within a few millimeters of the topsoil layer may develop biological soil crusts (BSCs), composed of cyanobacteria, green algae, fungi and many heterotrophic bacteria (Belnap, 2003). BSCs play key roles in colonizing barren substrates (Tirkey and Adhikary, 2005), biogeochemical cycling (Johansen, 1993; Brankatschk *et al.*, 2013) and plant colonization (Belnap and Harper, 1995). Oxygenic phototrophic microorganisms in desert crusts are essential participators in both carbon (C) and nitrogen (N) fixation (Belnap, 2002; Pointing and Belnap, 2012). Filamentous Cyanobacteria species of the genus *Microcoleus* and most often the species *M. vaginatus* are the keystones of BSCs (Zhang *et al.*, 2009; Abed *et al.*, 2010; Steven *et al.*, 2012a, 2012b), especially during early successional stages. Archaea normally constitute a minor component of desert organisms, but information about their compositions and functions in desert BSCs is very limited (Soule *et al.*, 2009; Steven *et al.*, 2013).

Terrestrial microbial communities are affected by many environmental factors including pH, soil moisture, nutrient availability and organic C content (Berg and Steinberger, 2008; Lindström and Langenheder, 2012); and spatial heterogeneity of populations has been found associated with soil depth and soil parent material in desert soils (Steven *et al.*, 2013). Additionally, in desert ecosystems, various physical disturbances may significantly influence spatial and temporal distribution of soil microbial communities, such as by sand burial (Rao *et al.*, 2012), trampling by animals (Kuske *et al.*, 2012) and wild fire (Hawkes and Flechtner, 2002). In erosional dune landforms, one primary physical disturbance is from wind regime, which exerts shear forces at soil surfaces, always gradually increasing along the stoss lope of a dune while dramatically declining along the lee slope (Kroy *et al.*, 2002). Because desert BSCs develop at the topsoil, they are likely susceptible to wind erosion, especially during their initial development. In the Kalahari Desert, BSC development can be restricted by burial by windblown sediment (Thomas and Dougill, 2007). Thus, we hypothesized that microbial communities in sand dunes might display spatial biogeographic patterns associated with dune landforms.

BSCs can be the dominant source of N for arid land ecosystems, especially for regions where rainfall and anthropogenic inputs of N are low (Belnap, 2002; Pointing and Belnap, 2012). Ammonium oxidation (the first step of nitrification) is a key transformation due to its role of 'biogeochemical hinge' in N cycling, linking N bioavailability and N loss (Johnson *et al.*, 2005). Two groups of microorganisms, ammonia-oxidizing archaea (AOA) and bacteria (AOB),

carry out this process in various terrestrial ecosystems (Ollivier *et al.*, 2011). Previous studies have shown that potential rates of ammonia-oxidation are comparable with the N_2-fixation rates measured in desert BSCs (Johnson *et al.*, 2005), and autotrophic microorganisms may dominate ammonia oxidation in desert soils (Marusenko *et al.*, 2013). However, it is still unclear whether AOA or AOB dominate ammonia oxidation in desert BSCs, and if distributions of ammonia-oxidizing populations are associated with sand dune landforms.

The aim of this study was to test the hypothesis that microbial communities display spatial distributions across different locations in dunes and to investigate the characteristics of ammonia oxidization in an arid desert soil. Sand dunes in the Gurbantunggut Desert, China were chosen as the study site. The bacterial and archaeal communities were studied using terminal restriction fragment length polymorphism (T-RFLP) and pyrosequencing approaches, and the abundances of Cyanobacteria, *Microcoleus*, AOA, and AOB were determined by quantitative PCR (qPCR).

Materials and Methods

Study site and sampling

Soil samples were collected in July 2012 from the southern part of the Gurbantunggut Desert which is located in the center of the Jungger Basin (44°11′-46°20′N, 84°31′-90°00'E), Xinjiang province of China. It is the second largest desert in China with an area of 48.8 thousand square kilometers. Fixed and semi-fixed dunes occupy 87% of the total area of the desert. Most dunes are in a direction of roughly NW–SE with heights of 15–20 m. Longitudinal sand dunes dominate the desert landscape. The annual precipitation ranges from 80 mm to 160 mm, whereas the mean annual evaporation is more than 2,000 mm. The mean annual temperature varies in a range of 6–10°C, with maximum temperature over 40°C. The total annual solar radiation in this region varies from 5692 to 6360 MJ/m^2, with 2780 to 2980 cumulative sunlight hours (Chen *et al.*, 2007). The winds in the desert are dominated by the westerly airflow and the northwest winds blowing off the Mongolian high pressure region. The wind speeds are greatest during late spring with an average of 11.17 m/sec (Zhang *et al.*, 2011). Few psammophytes including small arbors, shrubs and small semi-shrubs are widespread in the interdunal zones and the lower part of the stoss and lee slopes (Chen *et al.*, 2007).

The sampling was done at randomly selected four sand dunes spacing from each other by at least 1 km (dune 1#, 44°22′30.3″N, 87°55′24.9″E; dune 2#, 44°23′20.10″N, 87°54′44.80″E; dune 3#, 44°23′41.96″N, 87°53′59.42″E; dune 4#, 44°24′0.45″N, 87°54′41.03″E). The topsoils at a depth of 0–2 cm were sampled at the stoss slope (DS), lee slope (DL), dune crest (DC), and interdune (ID) from each of the sand dunes. At each sampling site, topsoils from three locations (about 30 cm apart) were collected and mixed evenly to obtain a representative sample for each site, and additional samples (approximately 300 g soils) from adjacent to the each sample soil were also separately taken for analysis of soil physicochemical properties. Soils were frozen on dry ice immediately after collection and stored at -20°C.

Physicochemical analyses

Chlorophyll a was extracted by 95% ethanol according to the method of Chen (2006). Other soil physicochemical characteristics were analyzed as follows. The soil pH and electrical conductivity (EC) value were measured in a 1:5 soil: water suspension. Total organic carbon content (TOC) was determined by the potassium dichromate oxidation method (Schumacher, 2002). Total nitrogen content (TN) was determined by Kjeldahl procedure, and ammonia and nitrate were determined with a spectrophotometer (Page, 1982; Yang *et al.*, 1998).

DNA extraction

Total DNA was extracted using the FastDNA SPIN kit for soil (Bio101 Systems, USA) facilitated with the FastPrep-24 bead beater system according to the manufacturer's instructions. The quantity and quality of DNA in the extracts were analyzed by using a nanodrop ND-1000 spectrophotometer (Thermo Scientific, USA) and agarose gel electrophoresis, respectively.

PCR amplification and T-RFLP

DNA from the soil samples were subjected to both bacterial and archaeal T-RFLP analyses as previously described (Yu *et al.*, 2010; Tang *et al.*, 2012). Archaeal and bacterial small subunit ribosomal RNA (SSU rRNA) genes were amplified for T-RFLP analysis using the universal archaeal primers Arch109F (5′-ACK GCT CAG TAA CAC GT-3′) and 5′ 6-carboxyfluorescein (FAM)-labeled Arch915R primer (5′-GTG CTC CCC CGC CAA TTC CT-3′) (Lueders and Friedrich, 2003), and the universal bacterial primers 5′ FAM-labeled 8F (5′-AGA GTT TGA TCC TGG CTC AG-3′) and 1492R (5′-CGG TTA CCT TGT TAC GAC TT-3′) (Dojka *et al.*, 1998), respectively. PCR amplifications were performed with an iCycler thermal cycler (Bio-Rad, USA). The PCR conditions were denaturation at 94°C for 5 min, followed by 25 cycles of denaturation at 94°C for 1 min, annealing at 50°C (for Archaea) or 51°C (for Bacteria) for (92-2(n-1)) sec for the n-th cycle (n=1, 2,…24), and extension at 72°C for 1.5 min (for Archaea) or 2 min (for Bacteria).

Purified archaeal and bacterial PCR amplicon were separately digested by *Taq*I and *Hha*I (TaKaRa), respectively. After desalting, the recovered DNA was mixed with formamide and a DNA fragment length internal standard, and denatured. The "Genescan" analysis was then conducted in a capillary electrophoresis system (ABI 3130 Genetic Analyzer, Applied Biosystems). Separated fragments were detected with ABI 3130 Collection version 2.7 and analyzed with GeneMapper Analysis Software (version 3.7). The relative peak area of each terminal restriction fragment (T-RF) was calculated by dividing the individual T-RF peak area by the total area of all peaks ranging from 50 to 900 bp.

454 amplicon pyrosequencing and data processing

SSU rRNA genes of bacteria and archaea were amplified from genomic DNA using primers 8F and 533R (5′-TTA CCG

CGG CTG CTG GCA C-3′) (Benitez-Paez *et al.*, 2013), and Arch344F (5′-ACG GGG YGC AGC AGG CGC GA-3′) (Raskin *et al.*, 1994) and Arch915R, respectively. Barcodes that allow sample multiplexing during pyrosequencing were incorporated into the 5′ end of primers 533R and Arch915R. PCR mixtures (20 µl) were prepared in duplicate each containing 10 ng of DNA template, 4 µl of 5×FastPfu buffer, 250 µmol/L of dNTPs, 0.8 µl of each 5 µmol/L primer and 0.4 µl FastPfu polymerase (TransGen AP221-02). The PCR conditions were as follows: 95°C for 2 min; 20 cycles at 95°C for 30 sec, 56°C for 30 sec, 72°C for 30 sec, and then 72°C for 5 min. Purified bacterial and archaeal PCR amplicons were pyrosequenced by Majorbio (China) using a Roche 454 FLX instrument (Roche Diagnostics, USA) and Titanium reagents.

Sequences were processed using QIIME v. 1.5.0 by selecting sequences with an average quality score >25, containing no ambiguous bases or homopolymers longer than six base pairs and avoiding any primer mismatches (Caporaso *et al.*, 2010b). And sequences were denoised using Denoiser (Reeder and Knight, 2010). Bacterial and archaeal operational taxonomic units (OTUs) were picked at a 97% similarity threshold using UCLUST and representative sequences were picked using the most abundant method before PyNAST aligning with the 16S rRNA Greengenes database aligned at 97% (DeSantis *et al.*, 2006; Caporaso *et al.*, 2010a; Edgar, 2010). Chimeras were identified using ChimeraSlayer and taxonomy was assigned using the RDP classifier with default settings (Wang *et al.*, 2007; Haas *et al.*, 2011). Sequence data have been submitted to the GenBank database under Bioproject Accession No. PRJNA232686.

Primer design and quantitative PCR

All available SSU rRNA sequences of *Microcoleus* cultured and as-yet-uncultured strains were retrieved from RDP release 10, Greengenes (DeSantis *et al.*, 2006), and the GenBank database. These sequences were added to the ARB database SSURef_106_SILVA_19_03_11_opt.arb (Pruesse *et al.*, 2007). Possible specific primers for *Microcoleus* spp. were designed using the ARB probe design program. The specificity of the primers was evaluated *in silico* with the BLAST search at the National Center for Biotechnology Information, and by cloning and sequencing of one soil sample. We designed a set of primer specifically for *Microcoleus* bacteria (Mc-F 5′-CTT TCC GAA GTT AAG CCC-3′ and Mc-R 5′-GGA ATT TTC CGC AAT GGG-3′). Total Cyanobacteria were quantified using a universal primer set CYA 359F (5′-GGG GAA TYT TCC GCA ATG GG-3′) and CYA 781R(a) (5′-GAC TAC TGG GGT ATC TAA TCC CAT T-3′) + CYA781R(b) (5′-GAC TAC AGG GGT ATC TAA TCC CTT T-3′) as previously described (Nubel *et al.*, 1997). Abundance of archaeal *amoA* genes were determined using the primers Arch-amoAF (5′-STA ATG GTC TGG CTT AGA CG-3′) and Arch-amoAR (5′-GCG GCC ATC CAT CTG TAT GT-3′) (Francis *et al.*, 2005), while bacterial *amoA* gene copy numbers were estimated using the primers amoA1F (5′-GGG GTT TCT ACT GGT GGT-3′) and amoA2R (5′-CCC CTC KGS AAA GCC TTC TTC-3′) (Rotthauwe *et al.*, 1997).

Quantitative PCR was performed in a 25 µl final reaction mixture volume consisting of 12.5 µl SYBR Premix Ex Taq (TaKaRa, China), 1 µl of each primer and 2 µl of properly diluted DNA template, and 0.25 mg/ml bovine serum albumin. PCR amplifications were carried out in 96-well optical plates on an Applied Biosystems 7300 qPCR system with 7300 SDS 1.4 software (Applied Biosystems) using the following protocols: 95°C for 1 min, 40 cycles of 10 sec at 95°C, 30 sec for annealing (at 53°C for *amoA* genes, and at 60°C for SSU rRNA genes of Cyanobacteria and *Microcoleus*), 1 min at 72°C and followed by plate reads at 83°C. Melting curve analysis was performed at the end of each real-time

Table 1. Physiochemical properties of the desert soils[a]

Sample[b]	pH	EC (Ds/cm)	Chl a (µg/g)	TN (%)	NO_3^- (µg/g)	NH_4^+ (µg/g)	TOC (µg/g)	Moisture (%)	w/v[c]
DC1#	7.7	138.2	ND[d]	0.01	2.6	13.7	19.2	0.05	1.58
DS1#	7.8	239.0	0.14	0.021	5.6	8.3	33.4	0.12	1.53
DL1#	8.3	153.3	0.047	0.019	2.6	6.7	19.6	0.09	1.55
ID1#	7.0	640.0	3.348	0.098	10.1	15.3	139.2	0.26	1.14
DC2#	8.1	119.7	ND	0.016	1.9	6.0	15.8	0.02	1.62
DS2#	7.8	200.8	ND	0.024	4.6	6.8	35.3	0.09	1.56
DL2#	7.8	139.7	ND	0.02	1.8	4.6	24.4	0.09	1.65
ID2#	7.3	177.0	0.93	0.036	6.0	5.5	55.4	0.13	1.41
DC3#	7.9	183.9	0.047	0.011	3.0	5.1	37.7	0.08	1.55
DS3#	7.6	299.0	0.279	0.028	7.0	4.2	71.3	0.20	1.52
DL3#	7.9	209.0	ND	0.021	2.8	5.4	29.0	0.18	1.62
ID3#	7.4	412.0	3.209	0.054	9.2	6.8	106.8	0.25	1.23
DC4#	8.2	136.5	0.047	0.013	1.7	4.9	19.6	0.07	1.59
DS4#	7.8	269.0	0.326	0.03	5.5	4.4	49.7	0.10	1.50
DL4#	8.3	136.0	0.326	0.015	1.9	4.8	20.6	0.08	1.57
ID4#	6.9	630.0	1.721	0.071	8.6	7.3	113.6	0.20	1.30

[a] Values are means of triplicate analysis.
[b] DS, stoss slope; DL, lee slope; DC, dune crest; ID, interdune.
[c] Ratios of soil dry weight to volume.
[d] ND, not detected.

PCR run to check the specificity of amplification products, before confirmation by standard agarose gel eletrophoresis. The standard plasmid carrying target genes was obtained by TA cloning and extracted using TIANpure Mini Plasmid kit (Tiangen, China). Standard curves were generated with serial dilutions (10 to 10^8 copies/μl) of the plasmids, and the threshold cycle values of unknown samples were plotted on the standard curves to determine the copy numbers of target sequences. All qPCRs were performed in triplicate.

Statistical analysis

The relative abundances of T-RF peaks in each sample were used as input for SPASS version 16.0 release, and Principal Component Analysis (PCA) was carried out based on the calculation of Euclidean distances. QIIME v.1.5.0 was used to calculate Chao1 richness estimator and Shannon diversity indices of each sample, and compare the community structures of archaea and bacteria among the soil samples with Principal Coordinates Analysis (PCoA). t-tests were performed to compare taxonomy abundance data, and correlation analysis of qPCR data with environmental factors was conducted using SPASS software with Pearson's correlation.

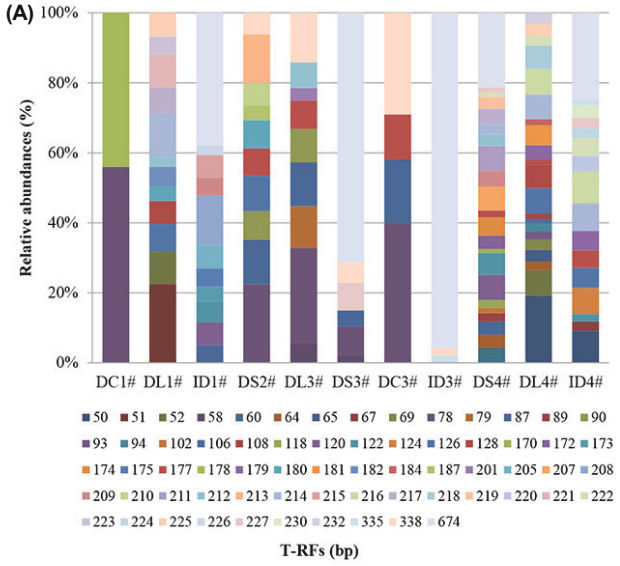

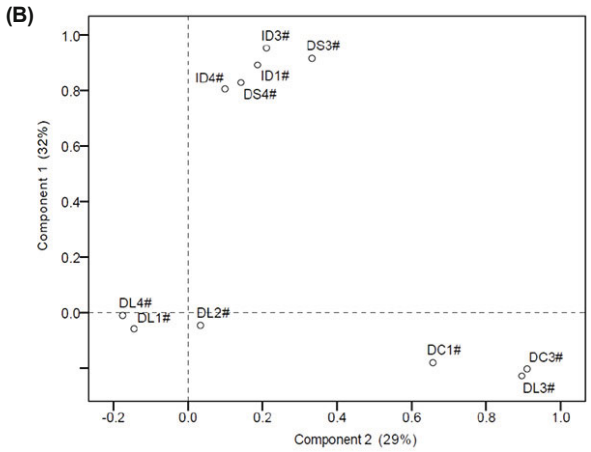

Fig. 1. Distribution bacterial T-RF peaks (A) and a Principal Component Analysis (PCA) plot (B) of bacterial communities in the desert soils (DS, stoss slope; DL, lee slope; DC, dune crest; ID, interdune). The relative abundances of each T-RF peak of each sample were used for the PCA analysis using SPASS 1.6 software.

Results

Physicochemical properties of the desert soils

The interdunal soil of each sampled dune exhibited the highest contents of chlorophyll a, DOC, total N, and nitrate N, while these corresponding components in soil from stoss slopes were higher than that from dune crest and lee slopes (Table 1). However, the interdunal soils had relatively low pH of 6.9–7.4, whereas soils from the other positions of the dunes had pH of 7.6–8.3 (Table 1).

T-RFLP analysis

Eleven soil samples were successfully PCR amplified and purified, and then T-RFLP was performed. T-RFLP analysis of bacterial communities (Fig. 1A) revealed high diversity in soils of the three positions of the 4# dune with 22, 21, and 16 T-RFs in DS4#, DL4#, and ID4#, respectively. In comparison, there were 2–12, 7 and 3–9 T-RFs in soils from the 1#, 2#, and 3# sand dunes, respectively (Fig. 1A). The taxonomic assignment of T-RF peaks of community samples was predicted by online analysis of software MiCA3 (http://mica.ibest.uidaho.edu/). T-RFs of 674 bp (representing Cyanobacteria) were dominant among the soils from interdunes and stoss slopes, while abundant T-RFs of 78 bp (representing *Arthrobacter* species) occurred in most other samples. PCA analysis of T-RFLP patterns showed that soil bacterial communities of the interdunes and stoss slopes clustered together with low variations, demonstrating the similarity of these communities (Fig. 1B). In contrast, T-RFLP analy-

Table 2. Diversity of bacterial and archaeal communities across the soil samples (DS, stoss slope; DL, lee slope; DC, dune crest; ID, interdune)

Sample[a]	Domain	No. of reads[b]	S_{chao1}	Observed species	Shannon
DC1#	*Bacteria*	15046	2976.12	1888	8.814
	Archaea	4617	473.363	300	4.715
DL1#	*Bacteria*	13586	3088.28	1873	8.903
	Archaea	3573	290.187	176	3.414
DL4#	*Bacteria*	4087	2392.99	1204	9.05
	Archaea	4439	253.177	132	3.215
ID1#	*Bacteria*	12360	4831.49	2738	9.233
	Archaea	4612	137.273	107	1.704
ID3#	*Bacteria*	5179	3642.32	1612	8.558
	Archaea	4917	185.172	121	1.932
ID4#	*Bacteria*	11163	4584.48	2620	9.517
	Archaea	4415	179.766	114	1.852
DS4#	*Bacteria*	4670	3005.09	1298	8.536
	Archaea	4665	148.02	100	1.927

[a] DS, stoss slope; DL, lee slope; DC, dune crest; ID, interdune.
[b] Reads that passed quality controls.

sis showed rather low diversity of archaeal communities with only 2-4 T-RFs (data not shown). Notably, T-RFs of 101 bp (representing members of Crenarchaeota) were common in these desert soils.

Pyrosequencing analysis

High-throughput deep sequencing was used to unravel the fine structure of prokaryotic communities. Based on the T-RFLP patterns, soil samples with high variability (three samples at 1# dune) and diversity (three samples at 4# dune) of bacterial populations as well as one interdunal sample (3# ID) were selected for pyrosequencing analysis.

A total of 66 091 high-quality bacterial 16S rRNA gene sequences were recovered across the soil samples, with an average of 9,441 sequences per data set (Table 2). All samples showed high bacterial diversity with Shannon indices in the range of 8.536–9.517 (Table 2). Consistent with the T-RFLP analysis, soils from the stoss slope and interdunes (named HC-BSCs, to indicate BSCs with a high abundance of cyanobacteria) had abundant cyanobacteria comprising 16.9–24.5% of bacterial communities, while the 16S rRNA gene pyrosequences from the crest and lee slope soils (named LC-BSCs, to indicate BSCs with a low abundance of cyanobacteria) contained 0.2–0.7% cyanobacterial sequences (Figs. 2A and 3). The majority of cyanobacterial sequences were classified into family Oscillatoriophycideae. Of these, *Microcoleus*-related sequences constituted 7.4–22% of the pyrosequencing reads in HC-BSCs, but were almost absent from LC-BSCs (Supplementary data Table S1); and a few *Chroococcidiopsis* and *Phormidium* species of the family were generally detected in HC-BSCs. In addition, a small number of sequences from 1# and 4# interdunes were assigned to family Nostocophycideae, and exhibited homology with heterocystous *Nostoc* spp.

Actinobacteria and Proteobacteria (especially Alphaproteobacteria) were commonly the dominant taxa across all soil samples (average abundance of 35.9 and 26.2%, respectively) followed by the phyla Bacteroidetes, Chloroflexi, Firmicutes, and Gemmatimonadetes (Figs. 2A and 3). However, cluster analysis based on the obtained pyrosequencing reads showed that the total bacterial communities of HC- and LC-BSCs were distinctly different (Fig. 4). There were significant differences (*t*-test, $P < 0.01$) between the two types of BSCs at different taxonomic levels. For example, a number of pyrosequencing reads from LC-BSCs were assigned into the phyla Bacteroidetes and Firmicutes; and more species in the orders Sphingobacteriales, Burkholderiales and Bacillales occurred in LC-BSCs. At the family level, Geodermatophilaceae was more abundant in HC-BSCs, whereas LC-BSCs had a significant wealth of Micrococcaceae, Sporichthyaceae, Chitinophagaceae, Flexibacteraceae, and Oxalo-

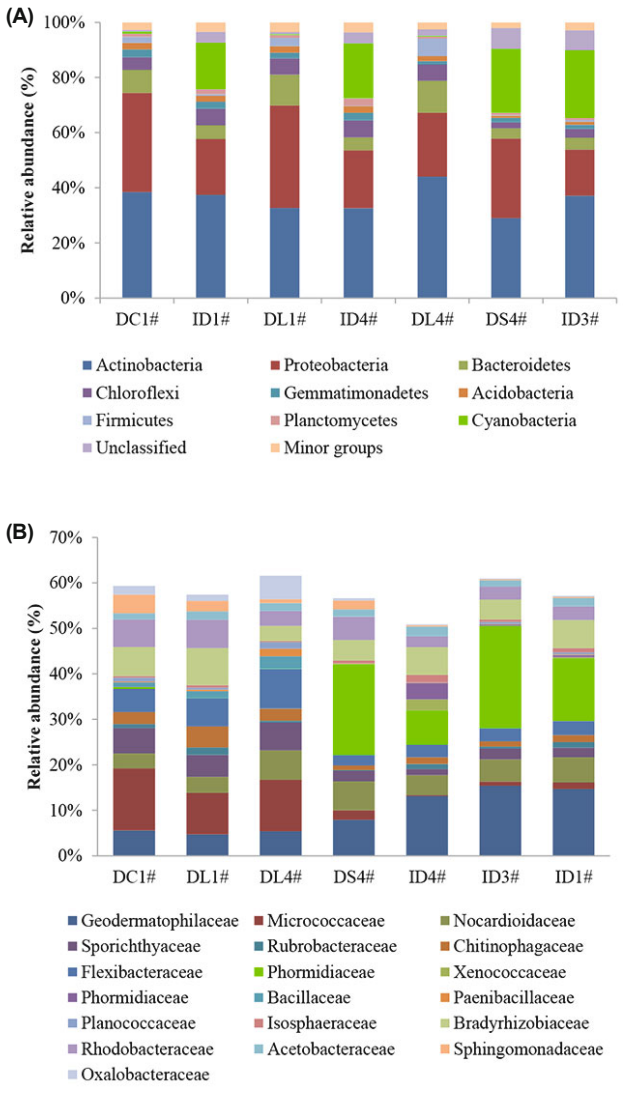

Fig. 2. Relative abundance of bacterial phyla (A) and identified major families (B) in the desert soils (DS, stoss slope; DL, lee slope; DC, dune crest; ID, interdune). Minor groups indicate the bacterial phyla with relative abundance ≦1.5%. Relative abundance of each major family is ≧1.5%.

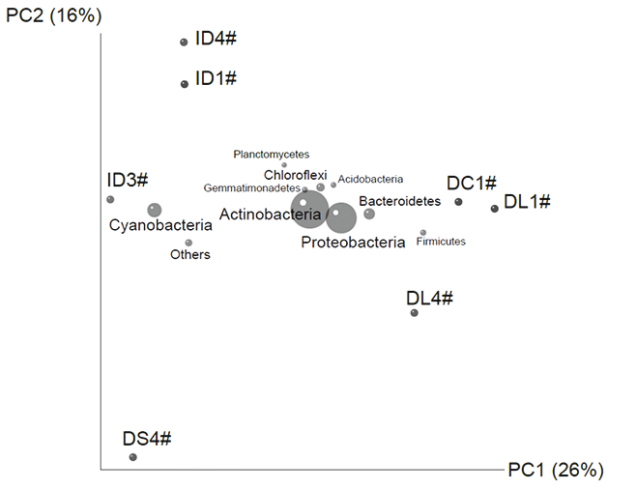

Fig. 3. A Principal Coordinate Analysis (PCoA) plot showing similarity of bacterial composition of desert soils. The coordinates of a given taxon are plotted as a weighted average of the coordinates of all samples, where the weights are the relative abundances of the taxon in the samples. The size of the sphere representing a taxon is proportional to the mean relative abundance of the taxon across all samples (DS, stoss slope; DL, lee slope; DC, dune crest; ID, interdune).

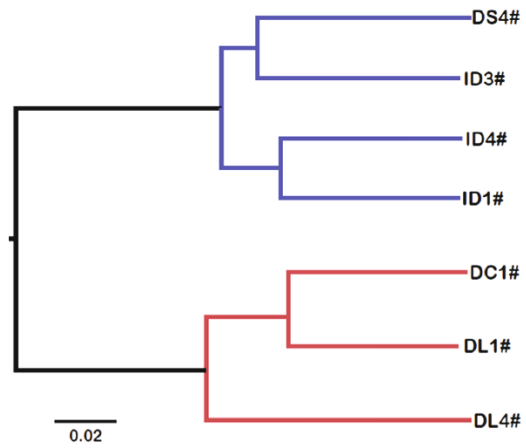

Fig. 4. A Unweighted Pair Group Method with Arithmetic mean (UPGMA) tree showing the relationship among the soil samples (DS, stoss slope; DL, lee slope; DC, dune crest; ID, interdune) based on the pyrosequencing data.

bacteraceae (Fig. 2B). In addition, Nitrosomonadaceae species, potential ammonia oxidizers (Ollivier *et al.*, 2011), were more frequently detected in LC-BSCs (Supplementary data Table S1).

A total of 31 238 high-quality archaeal 16S rRNA gene sequences were retrieved from the soil samples. Archaeal communities of the desert soils were less complex than the bacterial communities. In particular, HC-BSCs exhibited rather low diversity, with Shannon indices in the range of 1.704–1.932, compared to 3.215–4.715 for LC-BSCs (Table 2). Similar to the T-RFLP analysis, the majority of archaeal pyrosequencing reads, especially in HC-BSCs (99.4–100%), were classified into the phylum Crenarchaeota, and showed homology to *Nitrososphaera* spp. which are known to oxidize ammonia to nitrite in various soil ecosystems (Supplementary data Table S2) (Ollivier *et al.*, 2011). This implies that AOA may be involved in ammonia oxidation in this arid desert ecosystem. A number of pyrosequences (1.6–4.5%) from LC-BSCs were affiliated with class Thermoplasmata of Euryarchaeota. Most Thermoplasmata are thermophilic and acidophilic, and to our knowledge this is the first report of their presence in a desert soil ecosystem.

Quantitative PCR assay

Since the dominance of Cyanobacteria among soil bacterial communities at the interdunes and stoss slopes was revealed by both the T-RFLP and pyrosequencing analysis, the amount of total cyanobacteria in the soils was further quantified by qPCR. Meanwhile, due to the higher percentage of *Microcoleus*-like pyrosequencing reads in HC-BSCs, we developed a qPCR array to accurately quantify *Microcoleus* bacteria. On the other hand, as AOB and AOA were both detected by the pyrosequencing analysis of 16S rRNA genes, *amoA* genes of ammonia oxidizers were quantified to unravel the nitrification process in these desert topsoils. The 16S rRNA gene copy numbers of Cyanobacteria ranged from 2.93×10^4 to 1.57×10^{10} copies/g dry soil, which were at least two orders of magnitude higher in HC-BSCs than in LC-BSCs (Fig. 5A). Based on qPCR with primers designed for *Microcoleus* spp., the 16S rRNA gene copy number of *Microcoleus* was lower than that of Cyanobacteria except in the 4# DS sample. In most cases, *Microcoleus* was the predominant cyanobacteria in HC-BSCs with 34.6–119.9% of ratios of 16S rRNA gene copy numbers of *Microcoleus* to Cyanobacteria (Fig. 5A). Archaeal *amoA* gene copy numbers ranged from 3.55×10^5 to 4.02×10^8 copies per gram dry soil, and the interdunal samples had higher archaeal *amoA* gene abundances than soils from other positions in each dune. In contrast, bacterial *amoA* gene copy number (1.17×10^4 to 2.36×10^6 copies/g dry soil) was lower than that of archaea in each soil sample, especially in interdunal samples (Fig. 5B). The high ratios of archaeal to bacterial *amoA* genes in the interdunal soils (51 to 304) indicated that AOA might dominate the interdunal ammonia-oxidizing communities.

Correlation analysis

Pearson's moment correlation analysis demonstrated that chlorophyll a and gene copy numbers of *Microcoleus* and Cyanobacteria were strongly and positively correlated with the TN, NO_3^-, and TOC ($P < 0.01$), and were negatively correlated with pH ($P < 0.01$) (Table 3). In addition, chlorophyll a was significantly correlated with NH_4^+ and EC. These suggest that the growth of phototrophs may improve soil

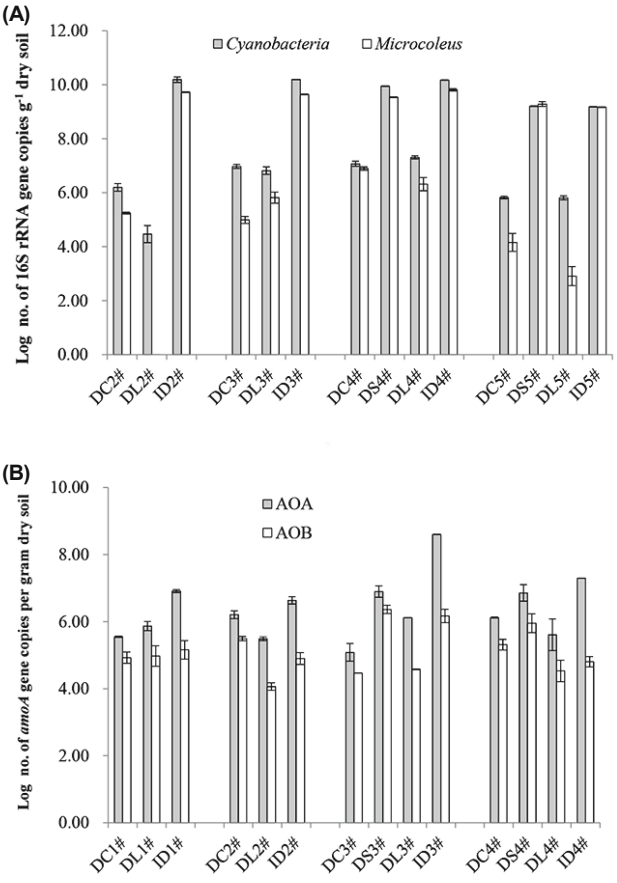

Fig. 5. 16S rRNA gene copy numbers of *Cyanobacteria* and *Microcoleus* (A), and abundances of archaeal and bacterial *amoA* genes (B) in the desert soils (DS, stoss slope; DL, lee slope; DC, dune crest; ID, interdune).

Table 3. Pearson correlation analysis of ammonia-oxidizing community structures with physicochemical parameters and cyanobacterial communities

Correlations	pH	EC	Chl a [a]	TN	NO_3^-	NH_4^+	DOC	AOA	AOB	Cyanobacteria	*Microcleus*	AOA/AOB	Moisture
pH		-0.840**	-0.743**	-0.841**	-0.864**	-0.451	-0.876**	-0.25	-0.156	-0.664**	-0.686**	-0.647*	-0.733**
EC			0.806**	0.947**	0.889**	0.45	0.955**	0.287	0.19	0.514	0.611*	0.691**	0.828**
Chl a				0.892**	0.834**	0.692*	0.901**	0.613	0.105	0.726*	0.796*	0.648*	0.880**
TN					0.875**	0.500*	0.952**	0.283	0.105	0.664**	0.715**	0.601*	0.813**
NO_3^-						0.371	0.949**	0.47	0.454	0.789**	0.877**	0.639*	0.865**
NH_4^+							0.402	0.01	-0.228	0.298	0.273	0.08	0.255
DOC								0.426	0.324	0.724**	0.804**	0.665**	0.884**
AOA									0.467	0.49	0.622*	0.625*	0.49
AOB										0.411	0.528	0.118	0.422
Cyanobacteria											0.960**	0.316	0.711**
Microcleus												0.434	0.781**
AOA/AOB													0.625*
Moisture													

[a] Chlorophyll a
* Correlation is significant at the 0.05 level (2-tailed).
** Correlation is significant at the 0.01 level (2-tailed).

fertility and affect microenvironments of the desert soil. Archaeal *amoA* genes and abundances of *Microcoleus* showed a significant positive correlation ($P < 0.05$), whereas the ratios of archaeal to bacterial *amoA* genes were negatively correlated with pH ($P < 0.05$).

Discussion

In this study, based on the culture-independent molecular approaches, the desert soil bacterial communities displayed specific distribution patterns associated with the landforms of sand dunes in the Gurbantunggut Desert. Soil samples collected from the stoss slopes and interdunes (HC-BSCs) showed similarity in bacterial communities, with high percentage of cyanobacteria (16.9–24.5%) that were mainly composed of *Microcoleus* spp. The higher chlorophyll a concentrations further supported the abundant cyanobacterial biomass for the stoss slopes and interdunes. In contrast, topsoils from the crest and lee slope exhibited some characteristics of early stages of successional BSCs, i.e. very small amounts of cyanobacteria (0.2–0.7%) with at least two orders of magnitude of 16S rRNA gene copies of Cyanobacteria (especially genus *Microcoleus*) lower than for other soil samples (Lan *et al.*, 2013). The harsh conditions at sand crests, including strong wind erosion and water evaporation, may be restrain colonization by cyanobacteria (Bowker *et al.*, 2006). Notably, despite similar soil moisture (Table 3), the soil bacterial communities at the stoss and leeward slopes were distinctly different; in particular, cyanobacteria were dense at stoss slopes. Wind disturbance possibly contributed to these differences. In a study of wind fluctuation over sand dunes in the Gurbantunggut Desert, Hu *et al.* (2011) found that the average wind velocity increased up the stoss slope, but rapidly decreased down the lee slope due to the existence of whirlpool. Wind force on the lee slope is sufficiently light for sand accumulation to lead to frequent sand burial events, a noticeable environmental disturbance in deserts (Belnap and Eldridge, 2003). In a field study on effects of sand burial stress on the early development of BSCs, Rao *et al.* (2012) reported that burial can impose severe stress on the growth of cyanobacteria in BSCs, such as the reduction of chlorophyll a and total carbohydrate reserve, as well as damaging activity of photosystem II. Thomas and Dougill (2007) also found that BSC development is restricted by burial with windblown sediment in the Kalahari Desert. Physical disturbance can greatly constrain the growth of *M. vaginatus* and other cyanobacteria in BSCs (Kuske *et al.*, 2012), reducing soil C available for often C-limited desert ecosystems (Belnap and Eldridge, 2003). Hence, although the buried cyanobacteria may lie dormant under the sand (Garcia-Pichel and Pringault, 2001), frequent burial by windblown sand might suppress the resurrection of buried cyanobacteria at the lee slopes in the Gurbantunggut Desert. Based on these results, it is suggested that fixing sand at dune crests by mechanical or physical sand fences may aid development of cyanobacterial crusts at lee slopes, thus improving soil fertility and promoting rehabilitation of the Gurbantunggut Desert.

Abiotic factors including soil pH, C content and moisture, as well as various disturbances may greatly impact microbial communities in desert soils (Belnap and Eldridge, 2003; Andrew *et al.*, 2012). Simultaneously, biotic factors also cannot be ignored. Yeager *et al.* (2004) proposed that development of mature biocrust requires bioengineering of the surface microenvironment by filamentous *M. vaginatus*. The qPCR analysis in the present study showed that abundances of *Microcoleus* spp. were significant correlated with many soil properties such as pH, EC, TN, and DOC (Table 3). This further supports the hypothesis that *Microcoleus* spp. can engineer the soil landscape which in turn shapes the microbial communities. There were significant differences between the two types of BSCs in some heterotrophic bacterial populations. HC-BSCs harbored a higher number of *Geodermatophilus* spp. (2.5–8.0%) than that in LC-BSCs (0.5–0.9%), implying that they had important roles during the formation of cyanobacterial crusts. Genus *Geodermatophilus* was first described by Leudemann (1968), and recently several strains have been isolated from deserts with various resistances such as xerotolerance, UV radiation-resistance and

halotolerance (Montero-Calasanz *et al.* 2012, 2013a–2013e). Cyanobacterial C-fixation might contribute to the frequent occurrence of heterotrophic *Geodermatophilus* bacteria in HB-BSCs. However, activities of *Geodermatophilus* bacteria could lead to the pH decline observed in the interdunes due to their acid-producing ability (Luedemann, 1968). By comparison, there was significantly abundant Micrococcaceae-like phylotypes showing homology with *Arthrobacter* spp. in LC-BSCs (7.3–10.8%) than in HC-BSCs (0.2–1.1%). Using cultivation-based method, Zhang *et al.* (2012) found that *Arthrobacter* comprised 12.8–69.5% of the total bacteria isolated from the Tengger Desert, China, and their abundances decreased from shifting sand dunes to fixed dunes depending on the degree of development of BSCs. These results suggested that *Arthrobacter* should be natural residents of desert soils. In addition, the abundances of *Bacillus* and *Segetibacter* were significantly higher in the LC-BSCs. Development of cyanobacteria, especially *Microcoleus* species, may greatly affect bacterial populations in the desert soils.

The archaeal diversity was extremely low in these desert crusts. The HC-BSCs showed less complex archaeal communities with Shannon indices $\leqq 2.0$, consisting almost entirely of potential AOA in *Nitrososphaera* (99.4–100.0%). Archaeal communities of LC-BSCs were also dominated by *Nitrososphaera* species, but contained more Halobacteriaceae and Thermoplasmata archaea. Potential AOB within family Nitrosomonadaceae were also detected in some LC-BSCs. *Nitrososphaera*-dominated archaeal communities suggest that archaea might be mainly involved in N cycling in these desert topsoils. In these desert soils, the NH_4^+ showed a close correlation with chlorophyll a ($P < 0.05$), indicating that phototrophs play important roles in the N input in desert ecosystems (Strauss *et al.*, 2012; Brankatschk *et al.*, 2013). Biocrust can be the dominant source of N in the Gurbantunggut Desert where rainfall inputs of N are low. However, comparable rates of ammonia-oxidation with N_2-fixation rates in many desert BSCs (Johnson *et al.*, 2005) indicate the important role of NH_4^+ oxidation in desert N-cycling. Thus, the amount of archaeal and bacterial *amoA* genes were compared by qPCR to understand this important process. The archaeal *amoA* gene was predominant in all soil samples, and was more abundant in the interdunal soils (10^6–10^8 copies/g dry soil). The ratios of archaeal to bacterial *amoA* genes ranged from 4 to 304, but with higher ratios for interdunes (51 to 304), suggesting that AOA possibly dominated the ammonia oxidization in interdunal BSCs. A similar phenomenon was observed by Brankatschk *et al.* (2013), in that the *amoA* gene abundance of AOA was 2–3 orders of magnitude higher than that of AOB in the biocrusts, and notably the abundance of AOA was matched by the nitrification activity pattern. In the present study, the archaeal *amoA* gene number was strongly correlated with the abundance of *Microcoleus* ($P < 0.05$). As discussed above, development of *Microcoleus* spp. accompanying the activities of other bacteria (e.g., *Geodermatophilus* spp.) possibly creates niches suitable for the growth of AOA. For example, pH of interdunal soils with abundant *Microcoleus* spp. was nearly neutral, while soils from other positions, especially crests and lee slopes, were alkaline in our study sites. The pH is an important factor shaping the distribution of ammonia oxidizing populations. Nitrification is primarily mediated by AOA under low as well as neutral pH conditions (Yao *et al.*, 2011), whereas AOB dominates the ammonia oxidation in alkaline soil (pH 8.3–8.7) (Shen *et al.*, 2008). Here, significantly negative correlations were found between the ratios of archaeal to bacterial *amoA* genes and pH values, suggesting that AOA plays a more important role than AOB in nitrification at the interdunes. Further *amoA* transcript analysis should provide more reliable evidence in future research.

In summary, our molecular analysis demonstrated that the distribution of soil microbial communities may be associated with the geomorphic characteristics of sand dunes in the Gurbantunggut Desert. The development of cyanobacteria (primarily *Microcoleus* spp.) in the desert topsoil could significantly change the soil bacterial composition, and positively correlated with ammonia-oxidizing archaea.

Acknowledgements

This work was financially supported by the Dean Fund of Graduate University of Chinese Academy of Sciences 2011B (Y15102FN00), the Strategic Priority Research Program of the Chinese Academy of Sciences (XDA05030500).

References

Abed, R.M.M., Al Kharusi, S., Schramm, A., and Robinson, M.D. 2010. Bacterial diversity, pigments and nitrogen fixation of biological desert crusts from the Sultanate of Oman. *FEMS Microbiol. Ecol.* **72**, 418–428.

Andrew, D.R., Fitak, R.R., Munguia-Vega, A., Racolta, A., Martinson, V.G., and Dontsova, K. 2012. Abiotic Factors Shape Microbial Diversity in Sonoran Desert Soils. *Appl. Environ. Microbiol.* **78**, 7527-7537.

Belnap, J. 2002. Nitrogen fixation in biological soil crusts from southeast Utah, USA. *Biol. Fer. Soils* **35**, 128–135.

Belnap, J. 2003. The world at your feet: desert biological soil crusts. *Front. Ecol. Environ.* **1**, 181–189.

Belnap, J. and Eldridge, D. 2003. Disturbance and recovery of biological soil crusts, pp. 363–383. Biological soil crusts: structure, function, and management, Springer.

Belnap, J. and Harper, K. 1995. Influence of cryptobiotic soil crusts on elemental content of tissue of two desert seed plants. *Arid Land Res. Manag.* **9**, 107–115.

Benitez-Paez, A., Alvarez, M., Belda-Ferre, P., Rubido, S., Mira, A., and Tomas, I. 2013. Detection of transient bacteraemia following dental extractions by 16S rDNA pyrosequencing: a pilot study. *PLoS ONE* **8**, e57782.

Berg, N. and Steinberger, Y. 2008. Role of perennial plants in determining the activity of the microbial community in the Negev Desert ecosystem. *Soil Biol. Biochem.* **40**, 2686–2695.

Bowker, M.A., Belnap, J., Davidson, D.W., and Harland, G. 2006. Correlates of biological soil crust abundance across a continuum of spatial scales: support for a hierarchical conceptual model. *J. Appl. Ecol.* **43**, 152–163.

Brankatschk, R., Fischer, T., Veste, M., and Zeyer, J. 2013. Succession of N cycling processes in biological soil crusts on a Central European inland dune. *FEMS Microbiol. Ecol.* **83**, 149–160.

Caporaso, J.G., Bittinger, K., Bushman, F.D., DeSantis, T.Z., Andersen, G.L., and Knight, R. 2010a. PyNAST: a flexible tool for

aligning sequences to a template alignment. *Bioinformatics* **26**, 266–267.

Caporaso, J.G., Kuczynski, J., Stombaugh, J., Bittinger, K., Bushman, F.D., Costello, E.K., Fierer, N., Pena, A.G., Goodrich, J.K., Gordon, J.I., and *et al.* 2010b. QIIME allows analysis of high-throughput community sequencing data. *Nat. Methods* **7**, 335–336.

Chen, L.Z., Li, D.H., Song, L.R., Hu, C.X., Wang, G.H., and Liu, Y.D. 2006. Effects of salt stress on carbohydrate metabolism in desert soil alga *Microcoleus vaginatus* Gom. *J. Integr. Plant Biol.* **48**, 914–919.

Chen, Y., Wang, Q., Li, W., and Ruan, X. 2007. Microbiotic crusts and their interrelations with environmental factors in the Gurbantonggut desert, western China. *Environ. Geol.* **52**, 691–700.

DeSantis, T.Z., Hugenholtz, P., Larsen, N., Rojas, M., Brodie, E.L., Keller, K., Huber, T., Dalevi, D., Hu, P., and Andersen, G.L. 2006. Greengenes, a chimera-checked 16S rRNA gene database and workbench compatible with ARB. *Appl. Environ. Microbiol.* **72**, 5069–5072.

Dojka, M.A., Hugenholtz, P., Haack, S.K., and Pace, N.R. 1998. Microbial diversity in a hydrocarbon- and chlorinated-solvent-contaminated aquifer undergoing intrinsic bioremediation. *Appl. Environ. Microbiol.* **64**, 3869–3877.

Edgar, R.C. 2010. Search and clustering orders of magnitude faster than BLAST. *Bioinformatics* **26**, 2460–2461.

Francis, C.A., Roberts, K.J., Beman, J.M., Santoro, A.E., and Oakley, B.B. 2005. Ubiquity and diversity of ammonia-oxidizing archaea in water columns and sediments of the ocean. *Proc. Natl. Acad. Sci. USA* **102**, 14683–14688.

Garcia-Pichel, F. and Pringault, O. 2001. Microbiology: Cyanobacteria track water in desert soils. *Nature* **413**, 380–381.

Haas, B.J., Gevers, D., Earl, A.M., Feldgarden, M., Ward, D.V., Giannoukos, G., Ciulla, D., Tabbaa, D., Highlander, S.K., and Sodergren, E. 2011. Chimeric 16S rRNA sequence formation and detection in Sanger and 454-pyrosequenced PCR amplicons. *Genome Res.* **21**, 494–504.

Hawkes, C.V. and Flechtner, V.R. 2002. Biological soil crusts in a xeric Florida shrubland: composition, abundance, and spatial heterogeneity of crusts with different disturbance histories. *Microb. Ecol.* **43**, 1–12.

Hu, Y., Wang, X., Guo, H., Zhao, X., Gai, S., and Yang, D. 2011. Wind fluctuation over semi-fixed longitudinal dune in gurbantunggut desert. *J. Desert Res.* **31**, 393–399 (In Chinese).

Johansen, J.R. 1993. Cryptogamic crusts of semiarid and arid lands of North America. *J. Phycol.* **29**, 140–147.

Johnson, S.L., Budinoff, C.R., Belnap, J., and Garcia-Pichel, F. 2005. Relevance of ammonium oxidation within biological soil crust communities. *Environ. Microbiol.* **7**, 1–12.

Kroy, K., Sauermann, G., and Herrmann, H.J. 2002. Minimal model for sand dunes. *Phys. Rev. Lett.* **88**, 054301.

Kuske, C.R., Yeager, C.M., Johnson, S., Ticknor, L.O., and Belnap, J. 2012. Response and resilience of soil biocrust bacterial communities to chronic physical disturbance in arid shrublands. *ISME J.* **6**, 886–897.

Lan, S.B., Wu, L., Zhang, D.L., and Hu, C.X. 2013. Assessing level of development and successional stages in biological soil crusts with biological indicators. *Microb. Ecol.* **66**, 394–403.

Lindström, E.S. and Langenheder, S. 2012. Local and regional factors influencing bacterial community assembly. *Environ. Microbiol. Rep.* **4**, 1–9.

Luedemann, G.M. 1968. Geodermatophilus, a new genus of the Dermatophilaceae (Actinomycetales). *J. Bacteriol.* **96**, 1848–1858.

Lueders, T. and Friedrich, M.W. 2003. Evaluation of PCR amplification bias by terminal restriction fragment length polymorphism analysis of small-subunit rRNA and *mcrA* genes by using defined template mixtures of methanogenic pure cultures and soil DNA extracts. *Appl. Environ. Microbiol.* **69**, 320–326.

Marusenko, Y., Huber, D.P., and Hall, S.J. 2013. Fungi mediate nitrous oxide production but not ammonia oxidation in aridland soils of the southwestern US. *Soil Biol. Biochem.* **63**, 24–36.

Montero-Calasanz, M.C., Goker, M., Potter, G., Rohde, M., Sproer, C., Schumann, P., Gorbushina, A.A., and Klenk, H.P. 2012. *Geodermatophilus arenarius* sp. nov., a xerophilic actinomycete isolated from Saharan desert sand in Chad. *Extremophiles* **16**, 903–909.

Montero-Calasanz, M.C., Goker, M., Broughton, W.J., Cattaneo, A., Favet, J., Potter, G., Rohde, M., Sproer, C., Schumann, P., Klenk, H.P., and *et al.* 2013a. *Geodermatophilus tzadiensis* sp. nov., a UV radiation-resistant bacterium isolated from sand of the Saharan desert. *Syst. Appl. Microbiol.* **36**, 177–182.

Montero-Calasanz, M.C., Goker, M., Potter, G., Rohde, M., Sproer, C., Schumann, P., Gorbushina, A.A., and Klenk, H.P. 2013b. *Geodermatophilus africanus* sp. nov., a halotolerant actinomycete isolated from Saharan desert sand. *Antonie van Leeuwenhoek* **104**, 207–216.

Montero-Calasanz, M.C., Goker, M., Potter, G., Rohde, M., Sproer, C., Schumann, P., Gorbushina, A.A., and Klenk, H.P. 2013c. *Geodermatophilus normandii* sp. nov., isolated from Saharan desert sand. *Int. J. Syst. Evol. Microbiol.* **63**, 3437–3443.

Montero-Calasanz, M.C., Goker, M., Potter, G., Rohde, M., Sproer, C., Schumann, P., Gorbushina, A.A., and Klenk, H.P. 2013d. *Geodermatophilus saharensis* sp. nov., isolated from sand of the Saharan desert in Chad. *Arch. Microbiol.* **195**, 153–159.

Montero-Calasanz, M.C., Goker, M., Potter, G., Rohde, M., Sproer, C., Schumann, P., Klenk, H.P., and Gorbushina, A.A. 2013e. *Geodermatophilus telluris* sp. nov., an actinomycete isolated from Saharan desert sand. *Int. J. Syst. Evol. Microbiol.* **63**, 2254–2259.

Nubel, U., Garcia-Pichel, F., and Muyzer, G. 1997. PCR primers to amplify 16S rRNA genes from cyanobacteria. *Appl. Environ. Microbiol.* **63**, 3327–3332.

Ollivier, J., Towe, S., Bannert, A., Hai, B., Kastl, E.M., Meyer, A., Su, M.X., Kleineidam, K., and Schloter, M. 2011. Nitrogen turnover in soil and global change. *FEMS Microbiol. Ecol.* **78**, 3–16.

Page, A.L. 1982. Methods of soil analysis. Part 2. Chemical and microbiological properties. American Society of Agronomy, Soil Science Society of America.

Pointing, S.B. and Belnap, J. 2012. Microbial colonization and controls in dryland systems. *Nat. Rev. Microbiol.* **10**, 551–562.

Pruesse, E., Quast, C., Knittel, K., Fuchs, B.M., Ludwig, W., Peplies, J., and Glöckner, F.O. 2007. SILVA: a comprehensive online resource for quality checked and aligned ribosomal RNA sequence data compatible with ARB. *Nucleic Acids Res.* **35**, 7188–7196.

Rao, B.Q., Liu, Y.D., Lan, S.B., Wu, P.P., Wang, W.B., and Li, D.H. 2012. Effects of sand burial stress on the early developments of cyanobacterial crusts in the field. *Eur. J. Soil Biol.* **48**, 48–55.

Raskin, L., Stromley, J.M., Rittmann, B.E., and Stahl, D.A. 1994. Group-specific 16S rRNA hybridization probes to describe natural communities of methanogens. *Appl. Environ. Microbiol.* **60**, 1232–1240.

Reeder, J. and Knight, R. 2010. Rapidly denoising pyrosequencing amplicon reads by exploiting rank-abundance distributions. *Nat. Methods* **7**, 668–669.

Rotthauwe, J.H., Witzel, K.P., and Liesack, W. 1997. The ammonia monooxygenase structural gene *amoA* as a functional marker: molecular fine-scale analysis of natural ammonia-oxidizing populations. *Appl. Environ. Microbiol.* **63**, 4704–4712.

Schumacher, B.A. 2002. Methods for the determination of total organic carbon (TOC) in soils and sediments. National ESD, ed.: EPA.

Shen, J.P., Zhang, L.M., Zhu, Y.G., Zhang, J.B., and He, J.Z. 2008. Abundance and composition of ammonia-oxidizing bacteria and ammonia-oxidizing archaea communities of an alkaline sandy loam. *Environ. Microbiol.* **10**, 1601–1611.

Soule, T., Anderson, I.J., Johnson, S.L., Bates, S.T., and Garcia-Pichel, F. 2009. Archaeal populations in biological soil crusts

from arid lands in North America. *Soil Biol. Biochem.* **41**, 2069–2074.

Steven, B., Gallegos-Graves, L., Belnap, J., and Kuske, C.R. 2013. Dryland soil microbial communities display spatial biogeographic patterns associated with soil depth and soil parent material. *FEMS Microbiol. Ecol.* **86**, 101–113.

Steven, B., Gallegos-Graves, L.V., Starkenburg, S.R., Chain, P.S., and Kuske, C.R. 2012a. Targeted and shotgun metagenomic approaches provide different descriptions of dryland soil microbial communities in a manipulated field study. *Environ. Microbiol. Rep.* **4**, 248–256.

Steven, B., Gallegos-Graves, L.V., Yeager, C.M., Belnap, J., Evans, R.D., and Kuske, C.R. 2012b. Dryland biological soil crust cyanobacteria show unexpected decreases in abundance under long-term elevated CO_2. *Environ. Microbiol.* **14**, 3247–3258.

Strauss, S.L., Day, T.A., and Garcia-Pichel, F. 2012. Nitrogen cycling in desert biological soil crusts across biogeographic regions in the Southwestern United States. *Biogeochemistry* **108**, 171–182.

Tang, Y.Q., Li, Y., Zhao, J.Y., Chi, C.Q., Huang, L.X., Dong, H.P., and Wu, X.L. 2012. Microbial communities in long-term, water-flooded petroleum reservoirs with different *in situ* temperatures in the Huabei Oilfield, China. *PLoS ONE* **7**, e33535.

Thomas, A.D. and Dougill, A.J. 2007. Spatial and temporal distribution of cyanobacterial soil crusts in the Kalahari: Implications for soil surface properties. *Geomorphology* **85**, 17–29.

Tirkey, J. and Adhikary, S. 2005. Cyanobacteria in biological soil crusts of India. *Curr. Sci. Bangalore* **89**, 515.

Wang, Q., Garrity, G.M., Tiedje, J.M., and Cole, J.R. 2007. Naive Bayesian classifier for rapid assignment of rRNA sequences into the new bacterial taxonomy. *Appl. Environ. Microbiol.* **73**, 5261–5267.

Yang, J., Kim, J., Skogley, E., and Schaff, B. 1998. A simple spectrophotometric determination of nitrate in water, resin, and soil extracts. *Soil Sci. Soc. Am. J.* **62**, 1108–1115.

Yao, H., Gao, Y., Nicol, G.W., Campbell, C.D., Prosser, J.I., Zhang, L., Han, W., and Singh, B.K. 2011. Links between ammonia oxidizer community structure, abundance, and nitrification potential in acidic soils. *Appl. Environ. Microbiol.* **77**, 4618–4625.

Yeager, C.M., Kornosky, J.L., Housman, D.C., Grote, E.E., Belnap, J., and Kuske, C.R. 2004. Diazotrophic community structure and function in two successional stages of biological soil crusts from the Colorado plateau and Chihuahuan desert. *Appl. Environ. Microbiol.* **70**, 973–983.

Yu, S.L., Tang, Y.Q., Li, Y., Zhang, H., and Wu, X.L. 2010. Gradient decrement of annealing time can improve PCR with fluorescent-labeled primers. *J. Biosci. Bioeng.* **110**, 500–504.

Zhang, B., Zhang, Y., Downing, A., and Niu, Y. 2011. Distribution and composition of cyanobacteria and microalgae associated with biological soil crusts in the Gurbantunggut Desert, China. *Arid Land Res. Manag.* **25**, 275–293.

Zhang, W., Zhang, G.S., Liu, G.X., Wang, L., Dong, X.P., Yue, J., Li, X.R., and An, L.Z. 2012. Characteristics of cultivable microbial community number and structure at the southeast edge of Tengger Desert. *Acta Ecologica Sinica* **32**, 567–577 (In Chinese).

Zhang, B.C., Zhang, Y.M., Zhao, J.C., Wu, N., Chen, R.Y., and Zhang, J. 2009. Microalgal species variation at different successional stages in biological soil crusts of the Gurbantunggut Desert, Northwestern China. *Biol. Fert. Soils* **45**, 539–547.